Nano-AlN Functionalization by Silane Modification for the Preparation of Covalent-Integrated Epoxy/Poly(ether imide) Nanocomposites

Jingkuan Duan,[1] Chonung Kim,[1,2] Pingkai Jiang,[1] Genlin Wang[1]

[1]*Shanghai Key Laboratory of Electrical Insulation and Thermal Aging, Shanghai Jiaotong University, Shanghai 200240, People's Republic of China*
[2]*Department of Electrical Engineering, Kim Chaek University of Technology, Pyongyang, Democratic People's Republic of Korea*

Received 22 September 2008; accepted 24 December 2008
DOI 10.1002/app.29962
Published online 26 October 2009 in Wiley InterScience (www.interscience.wiley.com).

ABSTRACT: Aluminum nitride nanoparticle (nano-AlN) organically modified with the silane-containing epoxide groups (3-glycidoxypropyltrimethoxy silane, GPTMS) was incorporated into a mixture of poly(ether imide) (PEI), and methyl hexahydrophthalic anhydride-cured bisphenol A diglycidyl ether grafted by GPTMS was prepared for nanocomposite. Scanning electron microscopy, transmission electron microscopy, and atomic force microscopy were used to investigate the microscopic structures of nanocomposites. According to experimental results, it was shown that addition of nano-AlN and PEI into the modified epoxy could lead to the improvement of the impact and bend strengths. When the concentrations of nano-AlN and PEI were 20 and 10 pbw, respectively, the toughness/stiffness balance could be achieved. Dynamic mechanical analysis (DMA) results displayed that two glass transition temperatures (T_g) found in the nanocomposites were assigned to the modified epoxy phase and PEI phase, respectively. As nano-AlN concentration increased, T_g value of epoxy phase had gradually increased, and the storage modulus of the nanocomposite at the ambient temperature displayed an increasing tendency. Additionally, thermal stability of the nanocomposite was apparently improved. The macroscopic properties of nanocomposites were found to be strongly dependent on their components, concentrations, dispersion, and resulted morphological structures. © 2009 Wiley Periodicals, Inc. J Appl Polym Sci 115: 2734–2746, 2010

Key words: nano-AlN; epoxy resin; poly(ether imide); nanocomposite; modification

INTRODUCTION

Thermoset epoxy resins are widely applied in adhesives, molding compounds, coatings, and composites because of their attractive combination of stiffness, strength, high heat distortion temperature, thermal and environment stability, creep resistance, and excellent processability. However, their brittleness inhibits further proliferation of the epoxy resin into various industrial applications. Therefore, many previous researchers have paid great attention to the subject of toughening the epoxy resins up to now.[1–3]

The bulk amount of epoxy resins, when used, is usually modified by the different approaches. There are many approaches used for toughening high-performance epoxy, which includes the following: (i) increasing the molecular weight of epoxy resin; (ii) lowering the crosslink density of matrix; (iii) incorporation of inorganic fillers into the pure epoxy, e.g., glass beads,[4] layered silicates,[5–8] and carbon nanotubes (CNTs),[9] and so on; (iv) chemical modification of the epoxy backbone for the improvement of flexibility, e.g., incorporation of some segments containing flexible groups into the molecules of epoxy[10–12]; (v) addition of a dispersed toughener phase to the cured polymer matrix. Some high-T_g, high-performance thermoplastics such as poly(ether imide) (PEI),[13,14] poly(ether ether ketone) (PEEK),[15] polysulfone (PSF),[16] rubbers and other elastomers[17,18] are blended to improve the toughness of the epoxy resins.

To open routes for the toughening of epoxy resins without any influence on the stiffness, strength, and glass temperature, three approaches and technologies have been adopted in this study: first, epoxy resin as the matrix resin has been modified by silane monomer-containing epoxide groups; second, a high-performance thermoplastic, PEI, with high thermal stability and remarkable modulus of elasticity and tensile strength has been used to toughen the modified epoxy; third, aluminum nitride

Correspondence to: G. Wang (allanshanghai@yahoo.com.cn).

Contract grant sponsor: Shanghai Committee of Science Technology; contract grant number: 05dz22303.

TABLE I
Formulation of Experiment

Samples	Epoxy (pbw)	MeHHPA (pbw)	Nd(III)AcAc (pbw)	AlN (pbw)	PEI (pbw)
EP331	51	49	0.2		
Modified331	51	49	0.2		
Modified331/AlN20	51	49	0.2	20	
Modified331/AlN10/PEI10	51	49	0.2	10	10
Modified331/AlN20/PEI10	51	49	0.2	20	10
Modified331/AlN35/PEI10	51	49	0.2	35	10
Modified331PEI10	51	49	0.2		10

nanoparticle (nano-AlN) functionalized by silane coupling agent has been used to toughen and strengthen the modified epoxy/PEI matrix.

Another objective of this article is to improve both toughness and strength of epoxy on the basis of exploring the toughness/stiffness balance. To our knowledge, there are few literatures that investigated the relationship between toughness and strength of the modified epoxy/nano-AlN/PEI composite; although development and application of thermoplastic and thermosetting nanocomposites filled with organically modified nanoscale materials have been the hot topics in recent years.[6,19]

In this study, the epoxy and the nano-AlN particle modified by silane containing epoxide groups have been synthesized and characterized by Fourier transform infrared spectroscopy (FTIR). The relationship between the microstructures of nanocomposites and their macroscopic properties have been explored by means of scanning electron microscopy (SEM), atomic force microscopy (AFM), transmission electron microscopy (TEM), dynamic mechanical analyses (DMA), and thermal gravimetric analysis (TGA). The results show that the macroscopic properties of the composites strongly depend on their microstructures.

EXPERIMENTAL

Materials

Diglycidyl ether of bisphenol A (DER 331) was received from Dow Chemicals Company, USA. Hardener used was methyltetrahydrophthalic anhydride (MeHHPA) obtained from Shanghai Li Yi Science and Technology Development, Shanghai, China. The Latent accelerator used was neodymium(III) acetylacetonate hydrate ((Nd(III)AcAc) purchased from Qinyang Tianyi Chemical, Qinyang County, China. Aluminum nitride (AlN) nanoscale particle was purchased from Hefei Kiln Naometer Technology Development, Heifei, China. The diameter of AlN particle is lower than 50 nm. The silane monomer (3-glycidoxypropyltrimethoxy silane, GPTMS) was purchased from Dow Corning Company, USA. The catalyzer, di-*n*-butyltin dilaurate was purchased from Beijing Zhengheng Chemicals Company, Beijing, China. The modifier, soluble PEI was synthesized elsewhere.[20,21]

Hybrid nanocomposites preparation

Preparation of the modified nano-AlN particle

The nano-AlN particle dried in a vacuum oven at 180°C for 24 h and appropriate amount of the silane (0.5–1 wt % based on the weight of AlN particle) were added into a 500-mL three-necked flask, equipped with a mechanical stirrer and a reflux condenser, and mixed in high-purity acetone (about 5 wt % based on the weight of silane) by stirring at 110–120°C for at least 4 h. After filtration, the silanized powders were dried in a vacuum oven at 120°C for 2 h to remove the solvent and the silane molecules that were not well bonded, and thus would not significantly contribute to the joint strength.

Synthesis of the modified epoxy

EP331 (30 g; 0.066 mol) in 100 mL of dimethylbenzene, 5.66 g of GPTMS (0.0256 mol, equals the mole amount of the hydroxyl group in EP331), and certain amount of organotin compound was taken into a 250-mL three-necked flask equipped with a mechanical stirrer and a reflux condenser, respectively. The mixture was allowed to react with stirring at 110–120°C for 4–5 h. The solvent and the byproduct alcohol were removed under a reduced pressure, and then a viscous colorless product was obtained.

Preparation of hybrid composites

The hybrid composite specimens were fabricated by means of the process suggested and used in many other studies,[22] which involves the use of a solvent. In this process, the modified331, latent catalyst, PEI, and/or modified AlN particles were weighted according to the formulation in Table I and dissolved in high-purity chloroform and mixed thoroughly by stirring for at least 10 min at ambient temperature, followed by sonication for 10 min.

Finally, a uniform mixture was obtained. The mixture was subjected to degassing at 100°C for 30 min to remove the solvent. Subsequently, a stoichiometric amount of MeHHPA was added to the mixture and stirred for 5 min at 100°C until it was completely dissolved. The resulting mixtures were cured in the open stainless steel molds for 4 h at 135°C and then postcured at 165°C for 14 h.

Characterizations and measurements

Fourier transform infrared spectroscopy

FTIR measurement was applied to characterize the AlN particle and unmodifed331 modified by GPTMS. The blends of nano-AlN and KBr powders were pressed into pellets by a hydraulic pressure machine. The pellets were measured with a Paragon 1000 (Perkin Elmer, USA) with the resolution of 4 cm^{-1}. The neat KBr pellets smeared by several milligrams of epoxy resin were measured under the same conditions.

Mechanical properties measurement

Bend test of the hybrid composites was determined by means of the electric tensile testing machine (Instron 4465; Instron, USA) at a crosshead speed of 0.5 mm/min and ambient temperature. Specimens for bend test were obtained according to ISO 178. The mechanical properties (bend modulus and strength) were determined from the load–elongation curves. Charpy impact test was carried out using a RAYRAN universal pendulum impact system at ambient temperature. Specimens for impact test were obtained according to ASTM D-256. At least eight samples were repeatedly tested for the identification of the bend and impact properties of each kind of nanocomposites, respectively.

Dynamic mechanical thermal analysis

The storage modulus and tan δ of the hybrid composites were measured with TA 2980 dynamic mechanical analyzer by using single cantilever mode. The geometry of specimens is 25 mm × 5.0 mm × 3 mm (length × width × thickness). Scans were conducted in a temperature range of 40–250°C at a heating rate of 3°C/min, and the frequency was 1 Hz.

Scanning electron microscopy

To observe the phase structure of the hybrid composites, the fracture surfaces of impact testing samples were coated with thin gold layers of about 100 Å. The fracture surfaces were examined by means of a JOL JSM 7401F field-emission scanning electron microscope (FESEM) at the activation voltage of 5.0 kV.

Atomic force microscopy

The specimens of hybrid composites for AFM observation were trimmed using a Leica Ultracut UCT ultramicrotome, the thickness of which was about 70 nm. The morphological observation of the samples was conducted on a Nanoscope IIIa scanning probe microscope (Digital Instruments, Santa Barbara, CA) in a tapping mode. A tip fabricated from silicon (45 μm in length with ca. 500 kHz resonant frequency) was applied for scanning, and the scanning rate was 2.0 Hz.

Transmission electron microscopy

The states of AlN particles and PEI dispersion in the hybrid composites were observed by means of TEM. Samples were cut using a Leica Ultracut UCT ultramicrotome. Microtomed thin sections were collected on 200-mesh copper grids and examined by a Philips CM300 TEM at 300 kV in bright field mode.

Thermal gravimetric analysis

To investigate the thermal stability of the hybrid composites, TGA measurements were performed using 5–10 mg of the hybrid composites at a heating rate of 10°C/min under nitrogen atmosphere, using a Cahn TG systems 41 thermogravimetric analyzer. The samples were subjected to TGA in high-purity nitrogen under a constant flow rate of 10 mL/min. Thermal decomposition of each sample occurred in a programmed temperature range 200–800°C.

RESULTS AND DISCUSSION

Modification of nano-AlN particle

It is well known that the investigation of polymer nanocomposites is faced with considerable challenges because of the nanoscale of the nanomaterial and concentration.[23] The main problems are in creating a good dispersion in the polymer matrix and a good interface between nanoparticles and the polymer matrix to achieve the load transfer necessary for enhanced mechanical response in high-performance polymers. Maintaining a strong nanomaterial/polymer interface and good dispersion are always crucial for good mechanical properties. However, a strong mismatch of the surface energy between AlN nanoparticles and epoxy resin causes the interface incompatibility and the poor dispersion, thus resulting in poor adhesion between them. These problems can be resolved through selectively

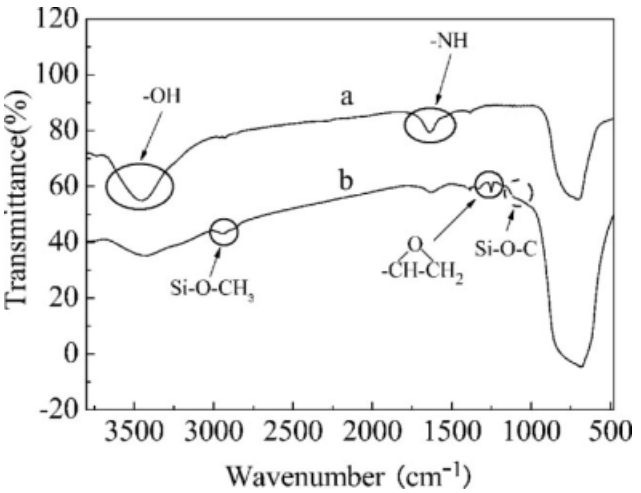

Figure 1 The FTIR spectra of (a) the raw AlN particles and (b) the GPTMS-modified AlN particle.

organofunctionalizing AlN nanoparticles, and subsequently binding them chemically to epoxy resin. The application of various silane surface-treatment agents[24] has been found to be effective for improving dispersion and adhesion between AlN nanoparticle and epoxy matrix, which also enhances the mechanical properties of the nanocomposites. There have been many reports that focus on the effects of coupling agents on the mechanical properties of epoxy composites.[25–27]

In this study, to enhance the dispersion and interface adhesion between AlN nanoparticles and epoxy matrix, a silane monomer, GPTMS, was chosen as coupling agent to functionalize AlN nanoparticles. Figure 1 gives the FTIR spectra of the raw and modified nano-AlN powders.

As shown in Figure 1(a), the raw nano-AlN particles show a much strong absorption at ν = 3200–3500 cm^{-1}, which may be attributed to hydroxyl group (—OH) peak stretching.[28] The band at ν = 1641 cm^{-1} is attributed to —NH— group vibration, which indicates that nano-AlN particles have higher affinity and reactivity to moisture and water. Therefore, the surface treatment has been undertaken to prevent the nano-AlN particles from hydrolyzing. The spectra of silane-modified AlN nanoparticles are very similar to those of raw nano-AlN particles, but some differences can still be detected. From Figure 1(b), the stretching vibration band of ether group is found in 1050–1150 cm^{-1} region. The band at 2990 cm^{-1}, attributed to methylene groups, is stronger than that of the raw nano-AlN particles. The absorption bands of epoxy groups at $\nu_{as}(CH_2)$ = 3003 cm^{-1}, $\nu_b(CH_2)$ = 1479 cm^{-1}, ν(C—O) = 1225 cm^{-1} can also be observed.[28] In addition, the absorption intensity of the bands at ν = 3200–3500 cm^{-1} and ν = 1641 cm^{-1}, which are assigned to hydroxyl group and amine group, respectively, can be found to apparently decrease. These changes of characteristic peaks indicated that GPTMS have already been grafted successfully on the surface of nano-AlN particles.

Modification of epoxy resin

If the silane monomer-containing epoxide groups is mixed simply into epoxy resin, the silane component may be dissolved and separated away from the curative systems in the course of curing. To overcome these drawbacks, the silane monomers have been grafted to epoxy resins before their usage by chemical modification via the reaction between hydroxyl group of epoxy resin and the alkoxy groups of silane. Commercial epoxy resin is chemically modified with silane monomer under the catalysis of organotin compound, aiming to enhance the toughness of epoxy matrix and to improve the compatibility between matrix and fillers. Figure 2 gives the FTIR spectra of GPTMS, modified331, and EP331.

As shown in Figure 2(c), the band at ν = 3200–3500 cm^{-1} is assigned to —OH stretching vibration. The bands at ν = 2970 and 590 cm^{-1} are characteristics of —CH_3 asymmetric and symmetric stretching, and the bands at ν = 2877 and 1461 cm^{-1} are assigned to —CH_2 asymmetric and symmetric stretching. The band at ν = 910 cm^{-1} is the characteristic absorption of epoxide groups. The absorption peaks at ν = 1604, 1520, and 828 cm^{-1} are attributed to substituted aromatic rings in unmodifed331. Some differences can still be detected in Figure 2(b), although the spectrum of the modifed331 is similar to that of EP331[29] as follows: (i) the peak intensity at about ν = 3200–3500 cm^{-1}, corresponding to —OH stretching vibration in epoxy resin, becomes weak

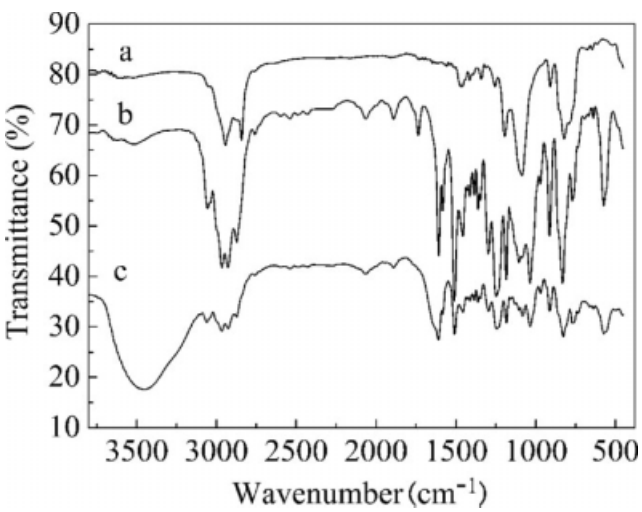

Figure 2 The FTIR spectra of (a) GPTMS, (b) modified331, and (c) EP331.

and even almost disappears after the silane modification, which reveals that hydroxyl groups are consumed by the graft reaction, resulting in a decrease in intensity; (ii) the peak intensity of low wavenumber region at $\nu = 500–2000\ cm^{-1}$ increases obviously because of the formation of Si—O—C bonds. These observations suggest that silane monomer has been successfully grafted to epoxy resin.

Morphology of the hybrid composites

The overall properties of a composite material were determined not only by the parent components but also by the phase morphology and interfacial properties of the composite. To analyze the dependence of the properties of hybrid composites on both structures and morphology, the SEM, TEM, and AFM measurements are employed in this study.

As shown in Figure 3(a), the fracture surface of EP331 is fine, rather smooth, and monotonous, except for some markings of river line near the crack initiation site, which resembles a typical brittle fracture mechanism, revealing that the resistance to crack propagation is very low. Also, the fracture surface of the modified331 is rougher, and the detailed surface features are more complex than that of EP331 [Fig. 3(b)], which displays the part toughness. Much rougher fracture surfaces and a greater number of dispersed phases are visualized in the samples of AlN-filled nanocomposites [Fig. 3(c–f)]. However, when the concentration of AlN nanoparticles is 35 pbw, large aggregates of AlN are observed in the modified331/PEI10 system, which could serve as the stress concentrations or crack initiators, leading to the premature and brittle failure. The modified331/PEI10 blend also displays a rougher fracture surface as shown in Figure 3(g). Therefore, some conclusions can be easily predicted from these SEM images as follows: (i) the modified331 epoxy by silane-containing epoxide groups could own higher impact toughness than the EP331 epoxy; (ii) the separate additions of nano-AlN particles and PEI into the modified331 epoxy could lead to toughness enhancement of the systems, respectively; (iii) nano-AlN particles and PEI would bring out synergistic effects to improve the toughness of the modified331/AlN/PEI systems; (iv) the excessive loadings of nano-AlN particles may result in the larger aggregates of fillers, which may lead to the poorer toughness in the modified331/PEI systems.

One of the most important questions in the nano-filled composites is the dispersion of fillers because nanoparticles dispersion in polymers can affect the final nanocomposite properties. Thus, to optimize nano-AlN particles dispersion in the modified331/PEI10 systems, it is necessary to investigate and quantify the dispersion, which can be done by visualizing the nano-AlN themselves, the interface, and the effect of the AlN on the surrounding matrix by means of TEM. Figure 4 displays TEM micrographs of the different nanocomposites.

As can be seen from Figure 4, nano-AlN powders in size of tens of nanometers are dispersed randomly in the epoxy matrix, and PEI is distributed as droplets or continuous regions in/between the epoxy matrix and nano-AlN powders. Additionally, nano-AlN powders are not fully located in one phase but migrate into the second component, which reveals that the nano-AlN particles modified by silane have excellent compatibility and good dispersion ability in the matrix and PEI. As the concentration of nano-AlN powders increases, the dispersion ability becomes poorer and poorer, especially, when the concentration of nano-AlN powders is 35 pbw, the size of aggregates of nano-AlN particles is about 200 nm [Fig. 4(c)]; below 20 pbw, nano-AlN powders are uniformly dispersed in the matrix and the size of the aggregates is less than 100 nm [Fig. 4(a,b)]. It can be seen from Figure 4(d) that epoxy phase and PEI phase are well bounded, and that there is a good interfacial adhesion between nano-AlN particles and polymer phase. Because silane-containing epoxide groups have been grafted to the surfaces of nano-AlN particles, there exist partial covalent bondings of nano-AlN particles to the polymeric network, which leads to the excellent compatibility between nano-AlN particles and polymeric matrix.

From Figure 4, it was found that the TEM images of nanocomposites display an obvious phase-separation structure resulting from two components of polymers that exist in the composite. PEI is segregated into spherical or continuous domains whose dimension is less than tens of nanometers and more than hundreds nm, respectively [see Fig. 4(b,c)]. According to our investigations[20,21] and previous literatures,[30,31] it may be possible for reaction-induced phase separation in the mixture of epoxy and PEI to occur, which can cause an increase in fracture toughness because the thermoplastic-rich phase allows the plastic deformation to be enhanced.

Figure 5 shows the AFM images of the modified331 and a representative modified331/AlN/PEI nanocomposite. The left and right images are the topography and phase contrast images, respectively. It is noted that the cured modified331 resin possesses the homogenous morphologies [Fig. 5(a)], whereas the distinguishable variation of morphology is observed in the modified331/AlN20/PEI10 blend, which displays microscopic phase separation [Fig. 5(b)]. The regions marked with the circularities could be ascribed to the AlN powders, which are well spread and incorporated in the interface between the organic and inorganic layers without any visible agglomeration.

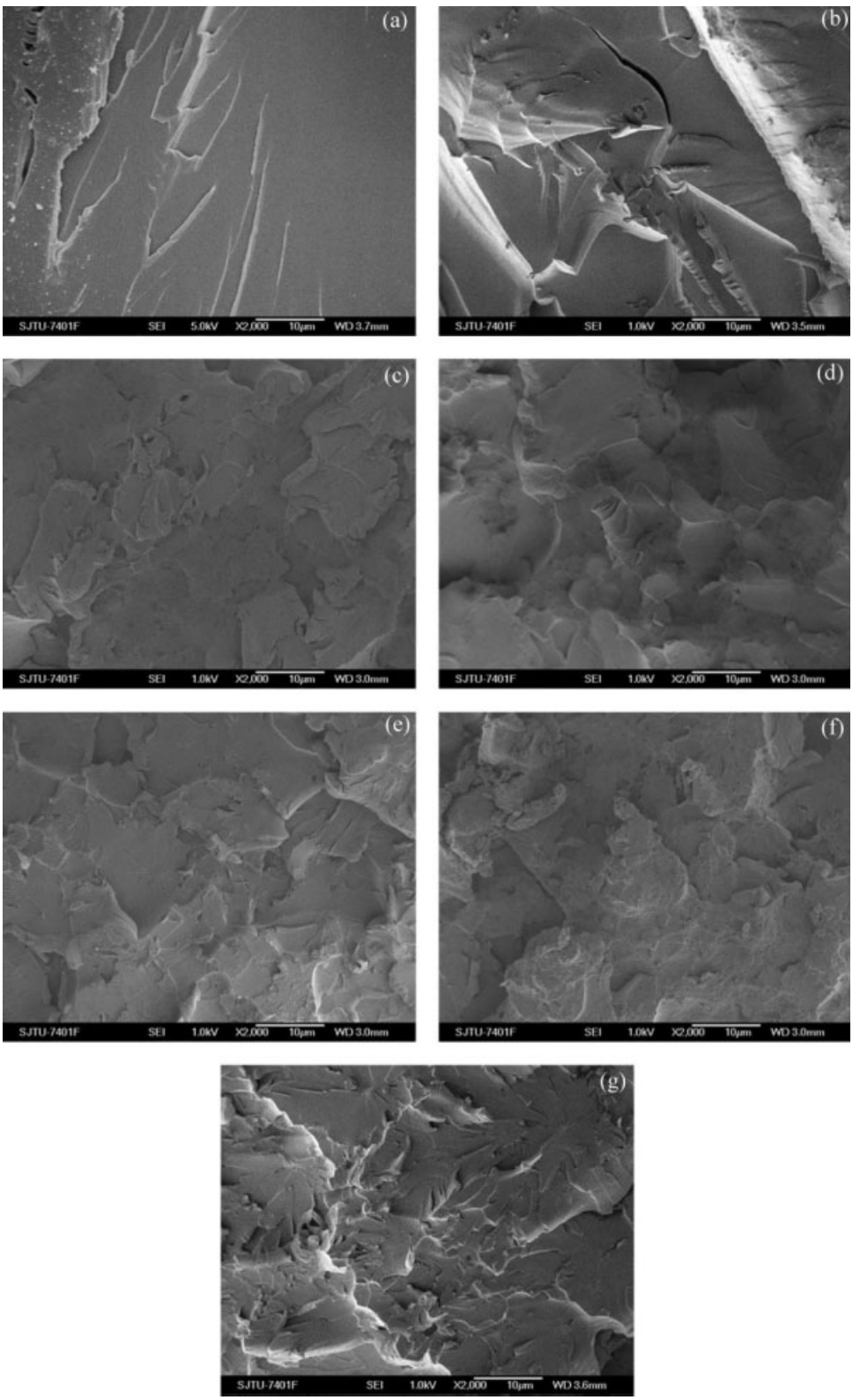

Figure 3 SEM micrographs of the impact fracture surfaces of the different composites: (a) EP331; (b) modified331; (c) modified331/AlN10; (d) modified331/AlN10/PEI10; (e) modified331/AlN20/PEI10; (f) modified331/AlN35/PEI10; and (g) modified331/PEI10.

The microscopic phase separation between epoxy matrix and PEI has been confirmed by AFM imagines. Thus a number of cavities can be seen in Figure 5(b). Such cavitation, followed by plastic deformation of the matrix, is believed to be the major toughening mechanism, which may be similar

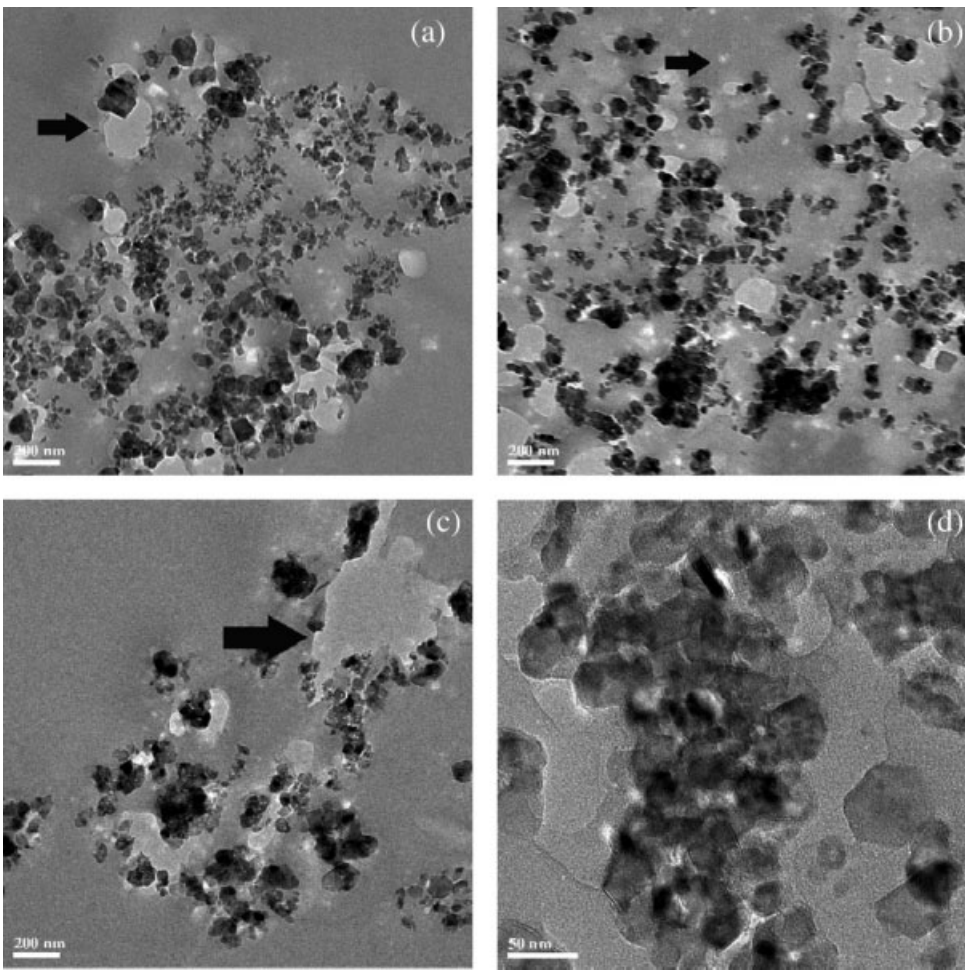

Figure 4 TEM micrographs of the hybrid nanocomposites: (a) modified331/AlN10/PEI10; (b) modified331/AlN20/PEI10; (c) modified331/AlN35/PEI10; and (d) the magnified micrograph of (b).

to the toughening mechanism of rubber modification thermosets.[32,33] Researchers agree that cavitation is not only a considerable source of toughening but also its importance on the plastic deformation of the matrix has been still widely recognized.[34] It has been widely accepted that the final mechanical properties of this mixture are determined by the phase structure. Generally, an interconnected or a bicontinuous phase-separated microstructure with fine domain sizes benefits the properties of the final products because both the toughness of thermoplastics and the stiffness of the thermosetting matrix can be combined.

Mechanical properties of the hybrid composites

Modulus and strength are key properties that basically decide the suitability of a material for usage in structural application. Figures 6 and 7 display the impact fracture strengths of the unmodified, modified epoxy and the hybrid composites. It should be noted from Figure 6 that the impact strength value of the modified331 is higher than that of the EP331, because the capacity for absorbing the fracture energy of —Si—O— segments in the modified331 molecules is greater than that of —C—O— segments in the EP331 molecules. In contrast to pure modified331, the impact strength value of the modified331/AlN20 blend slightly increases, which can be explained by the fact that the epoxide groups on the surface of AlN particles take part in the curing reactions of matrix, leading to the incorporation of —Si—O— segments on the surface of AlN particles into the networks of matrix. The addition of PEI into the modified331 results in the enhancement of the impact property because of the existence of high-performance thermoplastic (PEI) and phase separation in the modified331/PEI10 systems as shown in Figure 5. The impact strength of modified331/AlN20/PEI10 is up to 22.72 kJ/m^2 in contrast with 12.75 kJ/m^2 of EP331.

Additionally, the impact strength values of all modified331/AlN/PEI composites are higher than that of the modified331, showing significant toughening effects as shown in Figure 7. This may be ascribed to both the higher interfacial shear strength

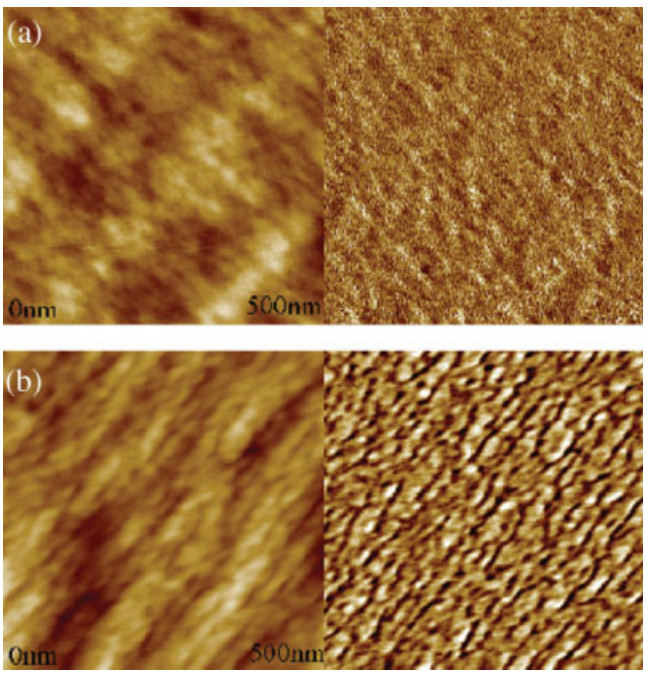

Figure 5 AFM images of (a) the modified331 and (b) the modified331/AlN20/PEI10. [Color figure can be viewed in the online issue, which is available at www.interscience.wiley.com]

of the chemical bonding between AlN particles and matrix and the crack deflection and/or plastic deformation of PEI phase. It is well known that the thermoplastic is located in isolated spherical domains and the dominant toughening mechanism is crack deflection. When the thermoplastic forms a continuous phase, the major toughening mechanism is changed from crack deflection to tearing-plastic deformation, which is known to be more effective. As seen in Figure 4, PEI displays the spherical and/or continuous domains, especially, in Figure 4(b). Thus, in the case of the systems studied here, the toughening mechanism can be considered to be crack deflection and/or tearing-plastic deformation. It is also

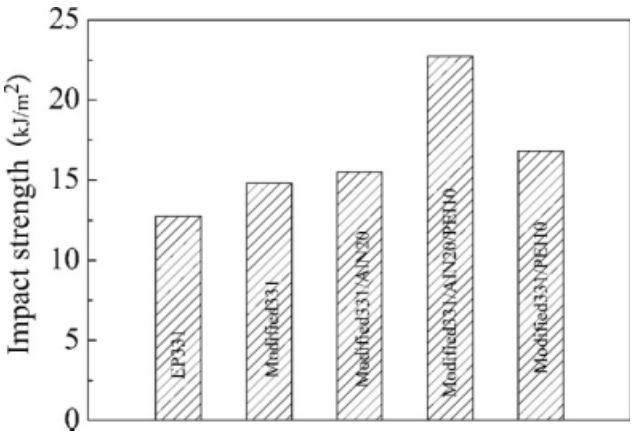

Figure 6 The impact strength of the different composites.

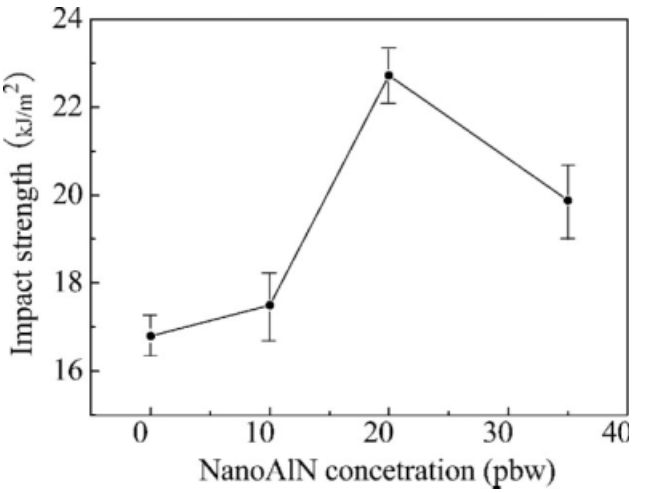

Figure 7 The impact strength of modified331/AlN/PEI10 composites as a function of AlN content.

found that in the range of 10–20 pbw, the higher the AlN concentrations, the greater is the impact strength, but above 35 pbw, the impact strength displays a slight reducing tendency. A few possible factors may contribute to the poor transfer of the impact strength when the inorganic filler content becomes high. One well-known explanation is that either the large aggregates of AlN particles restrain the crack deflection and/or plastic deformation zone size or fracture failure occurs in the filler/matrix interfacial zone and thus fracture failure takes place where the crack can propagate in AlN particles. From TEM images in Figure 4, the microaggregates of AlN particles become larger and larger with the increase of AlN concentrations. A relatively smaller toughening effect may occur because of the existence of the large segregated domains.[35,36] It is clearly found that AlN particles display the distinct agglomeration behavior when its content is at 35 pbw, which can serve as the stress concentrators that lead to premature and brittle failure. This has already been testified by the impact fracture SEM images in Figure 3(f).

Figure 8 gives the flexural modulus and bending strength of the modified331/AlN/PEI10 composites as a function of AlN concentration. From Figure 8, it can be clearly seen that the bending strength values of the modified331/AlN/PEI10 composites gradually increase with AlN concentration. In correspondence to the pure modified331, the flexural modulus values of the modifed331/AlN/PEI composites display a reducing trend at relatively lower concentration of AlN. However, they exhibit an increasing trend at relatively higher concentration of AlN. These results show the relationship of toughness/stiffness balance in the modified331/AlN/PEI10 composites. In general, the increase in toughness is accompanied by a decrease in stiffness for all hybrid

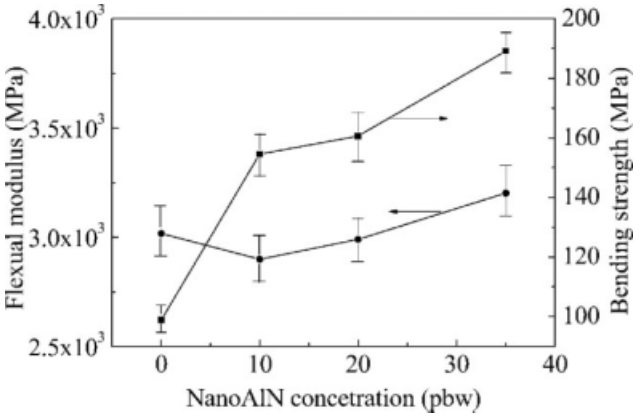

Figure 8 The flexural modulus and bending strength of modified331/AlN/PEI10 composites as a function of AlN concentration.

composites. The extent of toughness improvement also depends on the fillers concentration and additionally on the specific formulation of the various materials. In this study, all composites show a gradual increase in stiffness (due to gradual increase of the AlN powders concentration) with an almost unchanged toughness (due to the unchanged PEI concentration) in contrast with the pure modified331. When AlN and PEI concentrations are 20 and 10 pbw in the hybrid composite, respectively, the toughness/stiffness balance of hybrid nanocomposite is achieved, i.e., the flexural modulus value of hybrid nanocomposite is equal to that of pure modified331 resin. According to the toughness/stiffness balance, the hybrid nanocomposites with higher amount of AlN (more than 20 pbw) offer the best combination of significantly improved stiffness and almost unchanged toughness. On the other hand, these hybrid materials with lower AlN concentration (less than 20 pbw) display the combination of the improved toughness with only slightly increased stiffness.

When AlN concentration is higher than 20 pbw, the increase in stiffness is more pronounced, and when AlN concentration is lower than 20 pbw, the increase in toughness is more apparent, which leads to the changed trend of the flexural modulus values in Figure 8.

Characterizations of impact fracture behaviors and bending tests reveal that flexural modulus increases monotonically with the increasing of AlN concentration, while the fracture toughness shows a maximum at 20 pbw of AlN fillers in modified331/AlN/PEI systems.

The dynamic mechanical responses, e.g., the storage modulus and tan δ versus temperature diagram for the different composites are displayed in Figures 9 and 10. Figure 9(a) represents the changes in storage modulus (E') with a rise in temperature for EP331, the modified331, the modified331/AlN20, and the modified331/PEI10 composites. As clearly shown in Figure 9(a), the storage modulus at 40°C of the modified331 is higher than that of EP331, and the addition of AlN particles into the modified331 results in the increase in the storage modulus, whereas the addition of PEI leads to the decrease in the storage modulus of the modified331, which can be explained by the fact that the AlN particles modified by silane give an obstacle to the molecular mobility of epoxy, and that the PEI component increases the molecular mobility of epoxy. The storage modulus graphs show a sharp decrease in the temperature range 80–165°C, which correlates with the glass transition temperature.

As can be seen in Figure 9(b), the glass transition temperature (T_g) value of the modified331 is 116.6°C, which is lower than that of EP331. This may be ascribed to the substitution of —Si—O— segments for partial —C—O— segments in the modified331 molecules. It is well known that the mobility of —Si—O— segment is greater than that of —C—O— segment as the temperature increases. The modified331/AlN20

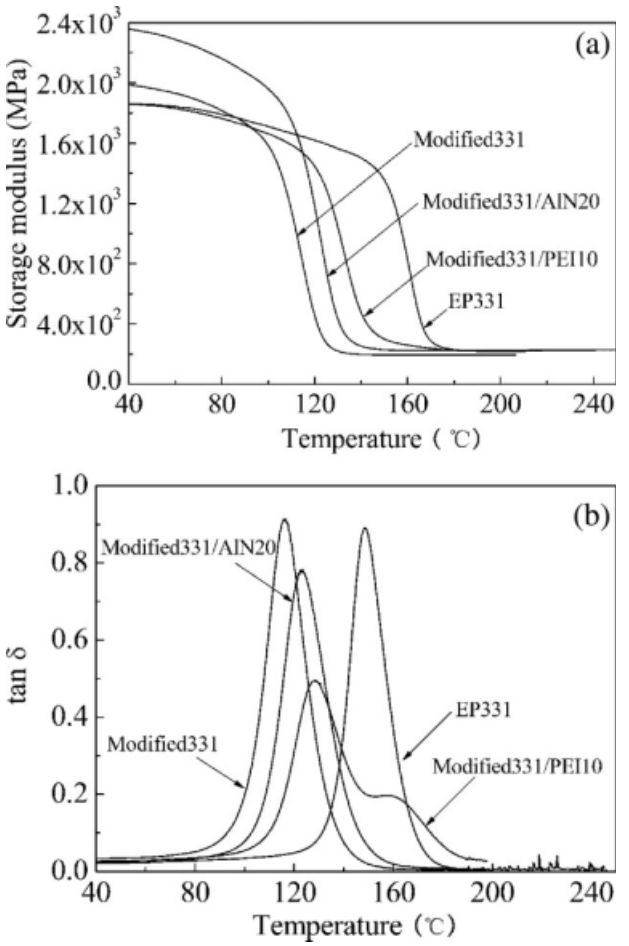

Figure 9 Storage modulus (a) and tan δ (b) versus temperature of the different composites.

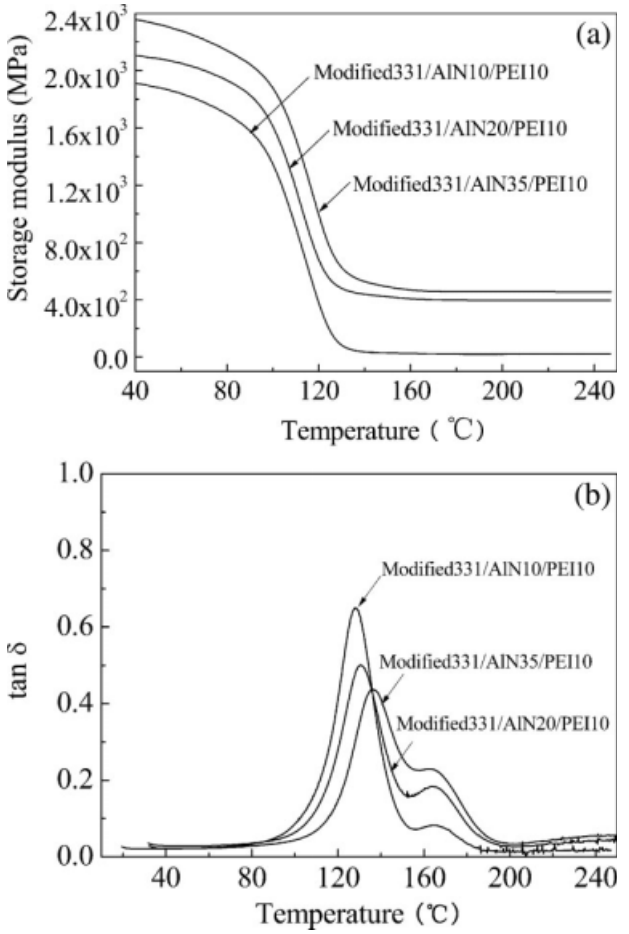

Figure 10 Storage modulus (a) and tan δ (b) versus temperature of the different modified331/AlN/PEI 10 composites.

composite exhibits a single higher temperature relaxation peak in comparison with the modified331, revealing that the addition of AlN particles into the modified331 gives an obstacle to the molecular mobility of epoxy because of the existence of the chemical bonds between the surface of AlN particles and epoxy molecules. On the contrary, the modified331/PEI10 composite displays two typical relaxation peaks as shown in tan δ curves, and they are centered at 128.5 and 163°C, corresponding to the glass transition temperatures of the epoxy phase and PEI phase, respectively, proving that they have the biphasic nature, which is in very good agreement with Figure 5. This can be interpreted by reaction-induced phase separation theory, which is well understood as an important physical/chemical theory in polymer science,[37,38] as follows: during reaction-induced phase separation, the chemical reaction and the physical phase-separation processes simutaneously take places. Before the curing reaction of epoxy resin, the system is miscible in the early period of the reaction, and no phase separation occurs. It was until the molecular weight of epoxy increase up to a certain value that the system becomes immiscible. Thus, the phase separation occurs in the resulting epoxy/PEI composite as shown in Figure 5(b).

According to the Fox equation,

$$\frac{1}{T_g} = \frac{\omega_1}{T_{g1}} + \frac{\omega_2}{T_{g2}} \quad (1)$$

It can be expected that the epoxy-rich phase of the 90/10 blend should contain ~44.5% PEI. The presence of one of the components in both phases of a binary blend can be due to either miscibility or chemical reactions between the components during curing or to both factors. The possibility of reactions between PEI and epoxy/anhydride seems unlikely, taking into account the chemical nature of both PEI and the curing mechanism of epoxy/anhydride/Nd(III)AcAc system. However, during curing, either slightly degraded molecules or end groups, aided by the presence of residual catalyst, can favor reactions. Thus, the modified331/PEI10 blend is composed of an almost pure PEI phase and an epoxy-rich phase where significant amounts of mixed PEI and slight amounts of reacted PEI are present.

Figure 10(a) indicates the changes in storage modulus with the rise in temperature. A change in the modulus indicates a change in rigidity, that is, a change in strength of a sample. It can be seen that the storage modulus of the nanocomposites increases in both glass and rubbery state with the increase in AlN content. The increase of modulus as a function of AlN loading means that AlN particles can serve as effective fillers to strengthen epoxy, which indicates that the incorporation of AlN has improved the stiffness of the nanocomposites. The drop in the storage modulus with temperature during the transition from the glassy state to the rubbery state occurs around 130°C, corresponding to the glass transition temperature of the switching segment. This drop in modulus is therefore ascribed to an energy dissipation phenomenon involving cooperative motions of long chains sequence.[39]

The damping property (tan δ) or the ratio of the dynamic loss modulus to the dynamic storage modulus is related to the molecular motions and phase transitions. Two important conclusions can be drawn from the relaxation peak shown in Figure 10(b).[40] First, it reflects the overall rigidity of the material. As shown in Figure 10(b), the value of the tan δ of the nanocomposites decreases with AlN concentration, revealing the increasing trend of rigidity of the nanocomposites. This is in good agreement with Figure 9. Second, the damping measurements also give practical information on the glass transition temperature. There are two well-defined glass transitions that appear in the modified331/AlN/PEI10

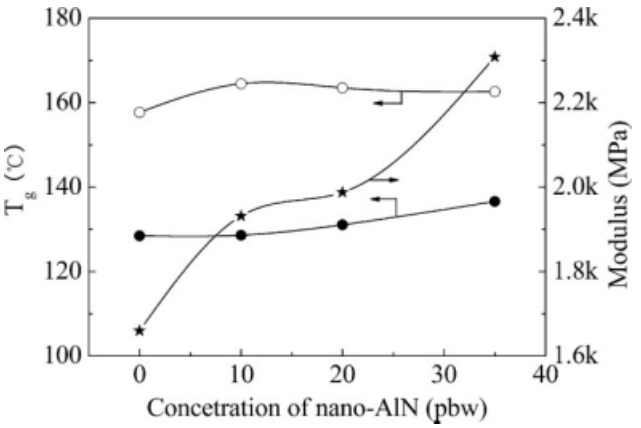

Figure 11 Glass transition behavior and modulus (at 30°C) of the modified331/AlN/PEI composites with the different concentrations of AlN obtained by DMTA. The filled symbols denote the T_g values of PEI phase; the open symbols represent those of the modified331 phase.

composites, which also proves their biphasic nature. The positions of the high-temperature glass transitions remain slightly changed at about 163°C and practically identical to the T_g value of PEI, indicating the presence of a nearly pure PEI phase. The low-temperature T_g shifts slightly toward higher temperatures as the AlN powder content increases, which reveals that the modified331/AlN/PEI10 composites have excellent thermal stability with increase of AlN filler loading.

Finally, it can be observed that the damping peak becomes broader with increase of AlN content. Such a phenomenon has also been reported in the previous research.[40] It is admitted that there exists a nonlinear relationship between the relaxation peak height and the concentration of AlN particles. It is assumed that the presence of fillers has increased the damping probably by either particle–particle friction where particles hold one another as in weak agglomerates or particle–polymer friction where there is no adhesion at the interface. This result is in good agreement with Figures 3 and 4.

A shift in T_g toward a higher temperature is due to the good interaction between AlN and epoxy, which restricts the mobility of the epoxy chain, as mentioned earlier. Because of the dispersion of AlN and the large interfacial area per unit volume between nanofillers and polymer, the AlN polymer nanocomposites own the higher modulus and strength.

Figure 11 summarizes the values of T_g and modulus (at 40°C) obtained from dynamic mechanical thermal analysis (DMTA) as a function of the concentration of AlN particles. The shifting of T_g can denote the strength of interaction between the two components of the blend and AlN particles in the molecular level. As can been in Figure 11, the T_g values of PEI phases in the nanocomposites are slightly higher than that in the modified331/PEI composite, which may be ascribed to the obstacle of AlN powders to the segment movement of PEI. It is worth noticing that the T_g values of PEI phases in the nanocomposites display a reducing tendency with increase of the AlN concentration, which may be attributed to the fact that higher AlN filler concentration results in poorer dispersion of the AlN nanoparticles in PEI phase because of the increase of viscosity. This result is in good agreement with those obtained by means of FESEM and SEM. There are two reasons why the T_g values of the modified331 phases display an increasing tendency with increase of the AlN concentration. First, higher the AlN filler concentration, greater is the obstacle to the segment movement of epoxy; second, the more intensive the covalent bonding between AlN particles and epoxy networks because of the existence of epoxide groups on the AlN nanoparticles modified by silane is, the stronger becomes the interaction between AlN particles and epoxy network. In accordance with the results of bending tests, the modulus values of the composites at 40°C are found to gradually increase with the increase of AlN loadings (Fig. 10). This shows a good agreement with the general rules shown in the polymer/inorganic filler composites. Several factors can play important roles in determining the performance properties, especially the mechanical behavior of the composite.

Thermal stability properties of the hybrid composites

From Figure 12, it is clear that the decomposition of EP331 begins to occur at about 300°C. The onset temperature of decomposition tends to slightly increase in most of the samples having different

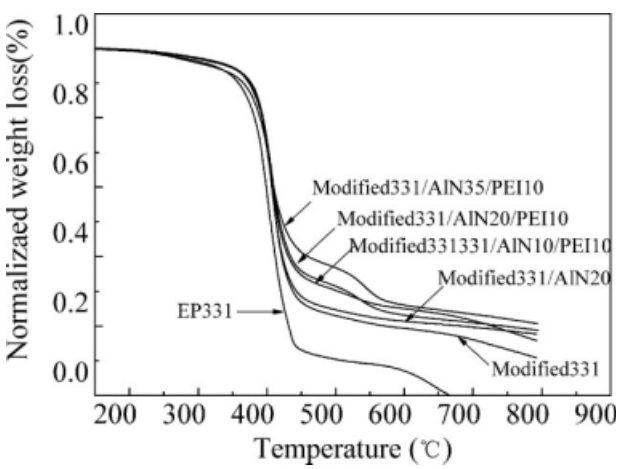

Figure 12 The experimental TGA curves of the different composites.

weight fractions of AlN nanofillers. The temperature for the full decomposition also shifts to a higher temperature. It is well manifested from Figure 12 that the modified331 loaded by AlN nanofillers has increased the thermal stability of the modified331/AlN/PEI nanocomposites, which may be explained by the fact that the higher heat capacity and thermal conductivity of AlN will cause it to preferably absorb the heat, resulting in the epoxy chains beginning to degrade at the higher temperature.[41] It was found that the thermal degradation temperature of the modified331 is higher than that of EP331, and that the increases in thermal degradation temperatures of the composites because of the addition of AlN particles and PEI revealed that the thermal stability of the composites has been improved. It can be explained that the active silane grafted on AlN particles improves the interacting forces between AlN nanoparticles and molecules of epoxy. Particularly, the epoxide groups of silane have taken part in the curing reaction of epoxy, so that the chemical bonds are formed between AlN nanoparticles and molecules of epoxy, which gives the obstacles to both the molecular mobility of matrix and the diffusion and penetration of low-weight molecules produced during the thermal degradation, thus leading to improvement of the thermal stability of the nanocomposite. Additionally, both the incorporation of —Si—O— segments in the networks of matrix and the rigid segments in PEI chain play important roles in improving the thermal stability.

CONCLUSION

In this study, the modified epoxy nanocomposites containing organophilically modified AlN nanofillers have been synthesized to combine the different properties of the individual components, so that both an improved toughness/stiffness balance can be achieved. The relationships between properties and structures of the hybrid nanocomposites have also been investigated in detail.

According to DMA measurements, two glass transition temperatures (T_gs) were observed in the hybrid nanocomposites, which are assigned to the modified epoxy phase and PEI phase, revealing that there may be reaction-induced phase separation phenomenon in the hybrid nanocomposites during curing process. This was proved by means of AFM images. With the increasing AlN nanoparticles concentration, T_g values of the modified phases gradually increase, and the storage modulus of the hybrid nanocomposites at room temperature displays an increasing trend. Mechanical measurements have shown that the addition of nano-AlN particles and PEI into the modified epoxy could lead to the improvement of the impacting and bending strength, and that when the concentrations of nano-AlN particles and PEI are 20 and 10 pbw, respectively, the toughness/stiffness balance can be achieved. The thermal stability of the hybrid nanocomposites were also significantly improved in comparison with the pure epoxy and modified epoxy. The macroscopic properties of the hybrid nanocomposites are determined by their components, concentration, dispersion, and the resulted morphological structure.

References

1. Riew, C. K.; Gillha, J. K., Eds. Rubber-Modified Thermoset Resins (Advances in Chemistry Series number 208); ACS: Washington, DC, 1984.
2. Riew, C. K.; Kinloch, A. J., Eds. Toughened Plastics I: Science and Engineering (Advances in Chemistry Series number 223); ACS: Washingtion, DC, 1993.
3. Riew, C. K.; Kinloch, A. J., Eds. Toughened Plastics II: Science And Engineering (Advances in Chemistry Series number 252); ACS: Washingtion, DC, 1996.
4. Xu, G.; Gong, M.; Shi, W. Polym Adv Technol 2005, 16, 473.
5. Koerner, H.; Hampton, E.; Dean, D.; Turgut, Z.; Drummy, L.; Peter, R. Chem Mater 2005, 17, 1990.
6. Frohich, J.; Thomann, R.; Mulhaupt, R. Macromolecules 2003, 36, 7205.
7. Koerner, H.; Jacobs, D.; Tomlin, D. W.; Busbee, J. D.; Vaia, R. D. Adv Mater 2004, 16, 297.
8. Utracki, L. A.; Sepehr, M.; Boccaleri, E. Polym Adv Technol 2007, 18, 1.
9. Breuer, O.; Sundararaj, U. Polym Compos 2004, 25, 630.
10. Gopala, A.; Wu, H.; Heiden, P. J Appl Polym Sci 1998, 70, 943.
11. Wu, H.; Xu, J.; Liu, Y.; Heiden, P. J Appl Polym Sci 1999, 72, 151.
12. Ochi, M.; Takahashi, R.; Terauchi, A. Polymer 2001, 42, 5151.
13. Bucknall, C. B.; Gillbert, A. H. Polymer 1989, 30, 213.
14. Marieta, C.; Remiro, P. M.; Garmendia, G.; Harismendy, I.; Mondragon, I. Eur Polym J 2003, 39, 1965.
15. Wang, X.; Lou, D. Y. S. Int J Engine Res 2003, 27, 377.
16. Mackinnon, A. J.; Jenkins, S. D.; McGral, P. T.; Petrick, R. A. Macromolecules 1992, 25, 3492.
17. Zheng, S.; Hu, Y.; Guo, Q.; Wei, J. Colloid Polym Sci 1996, 274, 410.
18. Ohsako, T.; Nagura, K.; Nozue, I. Polymer 1993, 34, 5080.
19. Bonnaud, L.; Pascault, J. P.; Sautereau, H.; Zhao, J. Q.; Jia, D. M. Polym Compos 2004, 25, 368.
20. Li, C. Master's Dissertation, Guilin University of Electronic Technology: Guilin, 2005 (in Chinese).
21. Duan, J. K. Master's Dissertation, Guilin University of Electronic Technology: Guilin, 2006 (in Chinese).
22. Lu, X.; Xu, G. J Appl Polym Sci 1997, 65, 2733.
23. Bower, C.; Rosen, R.; Jin, L.; Han, J.; Zhou, O. Appl Phys Lett 1998, 74, 3317.
24. Plueddemann, E. P. Silane Coupling Agent; Plenum Press: New York, 1991.
25. Pape, P. G.; Plueddemann, E. P. J Adhes Sci Technol 1991, 5, 832.
26. Morii, T.; Hamada, H.; Maekawa, Z.; Tanimoto, T.; Hirano, T.; Haruna, K. Polym Compos 1995, 16, 240.
27. Laura, D. M.; Keskkula, H.; Barlow, J. W.; Pau, D. R. Polymer 2002, 43, 4673.
28. Rahimi, A.; Gharazi, S.; Ershad-Langroudi, A.; Ghasemi, D. J Appl Polym Sci 2006, 102, 5322.
29. Ji, W.-G.; Hu, J.-M.; Liu, L.; Zhang, J.-Q.; Cao, C.-N. Surf Coat Technol 2007, 201, 4789.
30. Park, J. W.; Kim, S. C. Polym Adv Technol 1996, 7, 209.

31. Min, B. G.; Hodgkin, J. H.; Stachurski, Z. H. J Appl Polym Sci 1993, 50, 1065.
32. Kinloch, A. J. In Rubber-Toughened Plastics; Rview, C. K., Ed.; ACS: Washington, DC, 1989, Chapter 9.
33. Huang, Y.; Hunston, D. L.; Kinloch, A. J.; Bertsch, R. J.; Siebert, A. R. Adv Chem Ser 1993, 189.
34. Kang, B. U.; Jho, J. Y.; Kom, J.; Lee, S. S.; Park, M.; Lim, S.; Choe, C. R. J Appl Polym Sci 2001, 79, 38.
35. Zerda, A. S.; Lesser, A. J. J Polym Sci Part B: Polym Phys 2001, 39, 1137.
36. Becker, O.; Varley, R. J.; Simon, G. P. Polymer 2002, 43, 4365.
37. Gan, W. J.; Yu, Y. F.; Wang, M. H.; Tao, Q. S.; Li, S. J. Macromolecules 2003, 36, 7746.
38. Tao, Q. S.; Gan, W. J.; Yu, Y. F.; Wanf, M. H.; Tanf, X. L.; Li, S. J. Polymer 2004, 45, 3505.
39. Yu, S.; Hing, P. J Appl Polym Sci 2000, 78, 1348.
40. Razzaq, M. Y.; Frormann, L. Polym Compos 2007, 28, 287.
41. Luyt, A. S.; Molefi, J. A.; Krump, H. Polym Degrad Stab 2006, 91, 1629.